THE JOURNAL OF BIOLOGICAL CHEMISTRY VOL. 285, NO. 42, pp. 32539–32548, October 15, 2010

Tissue-nonspecific Alkaline Phosphatase Promotes the Neurotoxicity Effect of Extracellular Tau*

Received for publication, May 17, 2010, and in revised form, July 9, 2010 Published, JBC Papers in Press, July 15, 2010, DOI 10.1074/jbc.M110.145003

Miguel Díaz-Hernández[‡1], Alberto Gómez-Ramos[§¶1], Alicia Rubio[§¶1], Rosa Gómez-Villafuertes[‡], José R. Naranjo[¶‖], M. Teresa Miras-Portugal[‡], and Jesús Avila[§¶2]

From the [§]Centro de Biología Molecular "Severo Ochoa," Consejo Superior de Investigaciones Científicas-Universidad Autonoma de Madrid, 28049 Madrid, Spain, the [¶]Centro de Investigación Biomédica en Red sobre Enfermedades Neurodegenerativas (CIBERNED), 28049 Madrid, Spain, the [‡]Departamento de Bioquímica, Facultad de Veterinaria, Universidad Complutense de Madrid, 28040 Madrid, Spain, and the [‖]Centro Nacional de Biotecnología, Consejo Superior de Investigaciones, 28049 Madrid, Spain

There is solid evidence indicating that hyperphosphorylated tau protein, the main component of intracellular neurofibrillary tangles present in the brain of Alzheimer disease patients, plays a key role in progression of this disease. However, it has been recently reported that extracellular unmodified tau protein may also induce a neurotoxic effect on hippocampal neurons by activation of M1 and M3 muscarinic receptors. In the present work we show an essential component that links both effects, which is tissue-nonspecific alkaline phosphatase (TNAP). This enzyme is abundant in the central nervous system and is mainly required to keep control of extracellular levels of phosphorylated compounds. TNAP dephosphorylates the hyperphosphorylated tau protein once it is released upon neuronal death. Only the dephosphorylated tau protein behaves as an agonist of muscarinic M1 and M3 receptors, provoking a robust and sustained intracellular calcium increase finally triggering neuronal death. Interestingly, activation of muscarinic receptors by dephosphorylated tau increases the expression of TNAP in SH-SY5Y neuroblastoma cells. An increase in TNAP activity together with increases in protein and transcript levels were detected in Alzheimer disease patients when they were compared with healthy controls.

Alzheimer disease (AD)[3] is characterized by the loss of neurons and the presence of amyloid plaques and neurofibrillary tangles. The plaques are dense deposits of amyloid-β peptide and cellular material outside and around neurons, whereas the tangles are aggregates of the microtubule-associated protein tau, which has become hyperphosphorylated and accumulates inside the cells (1). In AD, tau pathology follows a reproducible pattern, in which hyperphosphorylated and aggregated tau first appears in the entorhinal cortex and hippocampus, and from there the disease spreads to the surrounding areas (2). During this process, neuronal loss occurs and tau protein may be found in the extracellular space in monomeric form or in aggregated form, assembled in extracellular ghost tangles. Indeed, an inverse correlation can be found between the number of extracellular tangles and the number of living neurons in the hippocampus (3–5). It has been also suggested that extracellular aggregated tau can promote the aggregation of intracellular tau (6). Moreover, it has been reported that extracellular monomeric tau is toxic for neurons, playing a role in the spreading of AD pathology (7–9). Monomeric tau-dependent toxicity occurs when extracellular tau binds and activates cell membrane receptors, identified as M1 and M3 muscarinic receptors (7).

Sluggish disassembly of aggregated tau and slow degradation of its monomeric form in extracellular media provide this protein with a long stay outside the cell. In this location, hyperphosphorylated monomeric tau can be recognized as a substrate of several extracellular enzymes, some of which can remove the phosphates from the protein (10, 11). One of these enzymes is tissue-nonspecific alkaline phosphatase (TNAP) (12), which possesses an alkaline optimum pH and is anchored to the membrane of different tissues (13). Some TNAP functions are well known, for example, playing an essential role in osteogenesis (14, 15), but its role in the central nervous system remains unknown.

The aim of this work was to study the whole process that follows the activation of muscarinic receptor by extracellular tau. We used human neuroblastoma cells instead of mouse cell lines because human tau has been shown to be more toxic than murine tau (16). We found that extracellular application of tau promoted neurodegeneration (9), facilitating release of intracellular tau into the extracellular medium where it becomes dephosphorylated by TNAP. We observed that only dephosphorylated tau promoted an increase in intracellular calcium levels in surrounding living cells, acting through membrane receptors, thus potentiating the toxic effect of tau. Moreover, dephosphorylated tau increased TNAP gene expression. Finally, the possible involvement of TNAP in the progression of AD was supported in analysis of samples from AD patients.

* This work was supported by Spanish Ministry of Health Grant SAF 2006-02424, CIBERNED Grant CB06/05/0035, Noscira Grant 2008/285, Comunidad de Madrid Grants SAL/0202/2006 and S-SAL-0253-2006, Spanish Ministry of Science and Education Grant BFU2008-02699, by the Fundación Marcelino Botín, Consolider SICI "Spanish Ion Channel Initiative" Grant CSD2008-00005, UCM-Santander Central Hispano Bank Grant 911585-670, and by an institutional grant from Fundación R. Areces.

[1] These authors contributed equally to this work.

[2] To whom correspondence should be addressed: Centro de Biología Molecular "Severo Ochoa," Universidad Autónoma de Madrid, C/Nicolás Cabrera 1, 28049 Madrid, Spain. Tel.: 34 91 196 45 64; Fax: 34 91 196 44 20; E-mail: javila@cbm.uam.es.

[3] The abbreviations used are: AD, Alzheimer disease; ACh, acetylcholine; BCIP/NBT, 5-bromo-4-chloro-3-indolyl phosphate/nitro blue tetrazolium; PP2A, protein phosphatase 2A; TES, *N*-tris(hydroxymethyl)methyl-2-aminoethanesulfonic acid; TNAP, tissue-nonspecific alkaline phosphatase.

TABLE 1

Details of control subjects and AD patients

In this study, six different samples of the medial temporal lobe from control and AD human brains were used. NBB number, age at death (years), sex (F: female; M: male), Braak stages (0–6), postmortem delay (in hours) and apoE genotype of control and AD brains used in this study are shown.

NBB number	Age at death	Sex	Braak stages	Postmortem delay	ApoE genotype
	years			*h*	
Controls					
03-040	73	F	0	4:00	3/2
03-061	83	F	1	5:30	3/2
05-083	85	F	1	5:00	
05-065	93	F	1	4:25	
05-019	74	M	3	5:00	4/3
04-060	85	M	1	4:15	4/4
AD					
00-089	70	F	6	4:30	3/3
00-140	72	F	6	3:45	4/3
94-025	85	F	6	5:00	3/3
96-066	91	F	6	4:35	4/3
95-069	68	M	6	4:15	4/4
01-091	73	M	6	5:00	4/3

EXPERIMENTAL PROCEDURES

Antibodies and Reagents—Atropine, levamisole, acetylcholine, and bovine kidney TNAP were purchased from Sigma-Aldrich. The following antibodies raised against tau protein were used: polyclonal BR133 antiserum (from Dr. C. Wischik, University of Aberdeen), monoclonal PHF1 antibody (from Dr. P. Davies, Albert Einstein College of Medicine), monoclonal AT8 antibody (Innogenetics, Gent, Belgium), monoclonal Tau-1 antibody (Chemicon, Temecula, CA), and monoclonal Tau-5 antibody (Calbiochem). BR133 recognizes the N-terminal region of tau protein. PHF1 recognizes tau phosphorylated at Ser^{396} and Ser^{404} (17), whereas AT8 recognizes tau when it is phosphorylated at Ser^{202} and Thr^{205}. Finally Tau-1 recognizes tau when it is not phosphorylated at Ser^{198}, Ser^{199}, and Ser^{202}; and Tau-5 is a phosphate-independent antibody that recognizes total amounts of tau protein. Other antibodies were also employed: polyclonal TNAP antiserum (Abcam, Cambridge, MA), monoclonal DM1A antibody that recognizes the α-subunit of tubulin (Sigma-Aldrich), monoclonal PP2A antibody that recognizes the catalytic subunit of protein phosphatase 2A (BD Transduction Laboratories, San Jose, CA), polyclonal NMDA antibody that recognizes the subunit 2C of NMDA receptors (Invitrogen), and Hsp90 antibody (Stressgen, Ann Arbor, MI).

Human Brain Samples—Human brain tissues were obtained from The Netherlands Brain Bank, which supplies postmortem specimens from clinically well documented and neuropathologically confirmed AD patients and nondiseased donors (NBB, Netherlands Institute for Neuroscience, Amsterdam, Coordinator, Dr. I. Huitinga). The NBB works in accordance with all national laws and regulations. Frozen samples used were obtained from three different regions of the temporal lobe (inferior, medial, and superior) from six nondemented controls and six patients with the clinical diagnosis of AD (Table 1).

Cell Cultures—SH-SY5Y human neuroblastoma cells (18), obtained from American Type Culture Collection (Rockville, MD), were grown in Dulbecco's modified Eagle's medium (DMEM) supplemented with 10% fetal bovine serum (v/v; FBS), 2 mM glutamine, and 50 mg/ml gentamicin (all from Invitrogen) in a humidified atmosphere with 5% CO_2. The day before performing the experiment, cells were seeded onto 15-mm^2 glass coverslips precoated with 1 mg/ml poly-L-lysine at a density of 1×10^5 cells/coverslip for calcium assay experiments and immunocytochemical studies. For immunocytochemical experiments, SH-SY5Y cells were cultured in free-serum medium for 48 h in the presence of 10 μM retinoic acid (Sigma-Aldrich). For Western blotting experiments, cells were seeded onto 6-well plates and exposed to tau proteins for 48 h.

Purification and Synthesis of Proteins and Peptides—The tau3RC fragment containing first, third, and fourth microtubule binding domains plus the C-terminal end of tau42 protein was isolated as previously described (19). Tau42, the longest tau isoform present in the central nervous system with four microtubule binding domains and two N-terminal inserts (20), was obtained similarly (19). Using an analogue protocol, hyperphosphorylated tau was purified from two different biological sources: SH-SY5Y cells treated with 10 μM okadaic acid for 1 h at 37 °C or an insect cell culture infected with baculovirus-expressing tau protein (21). For some experiments, hyperphosphorylated tau was dephosphorylated by TNAP treatment. Briefly, hyperphosphorylated tau was incubated with one enzyme unit of TNAP for 1 h at 37 °C in PBS buffer, pH 9.8. After dephosphorylation, the mixture was boiled for 5 min to inactivate the enzyme. All proteins were characterized by gel electrophoresis followed by staining with Coomassie Blue. Peptides $tau_{391-404}$ (EIVYKSPVVSGDTSPRH) and phospho-$tau_{391-404}$ (containing the same sequence, but with all serine residues phosphorylated) were synthesized and purified as previously reported (22). All of the references to the numbering of tau amino acid residues are based in the longest human tau isoform present in the central nervous system with two N-terminal inserts and four microtubule binding domains (20).

Western Blot Immunoassay—SH-SY5Y cells were washed with PBS, harvested, and boiled for 5 min in electrophoresis sample buffer supplemented with 30 mM glycerophosphate, 5 mM pyrophosphate, 1 μM okadaic acid, and a mixture of protease inhibitors (1 mM phenylmethanesulfonyl fluoride, 10 μg/ml leupeptin, 10 μg/ml aprotinin, and 50 μg/ml pepstatin; Roche Applied Science). Hyperphosphorylated tau treated or not treated with TNAP was similarly boiled in electrophoresis buffer. Proteins were separated by SDS-PAGE on 10% gels and transferred to nitrocellulose membranes (Schleicher & Schuell). After blocking nonspecific protein binding to the membranes with PBS containing 0.05% Tween 20 (v/v) and 5% nonfat dry milk (w/v), membranes were incubated overnight at 4 °C with the following primary antibodies diluted in blocking buffer: tau-5 (1:1000), Br133(1:100), Tau-1 (1:5000), PHF1 (1:100), AT8 (1:100), TNAP (1:200), PP2A (1:1000), NMDA (1:100), Hsp90 (1:1000), and DM1A (1:1000). Bands were visualized by enhanced chemiluminescence (PerkinElmer Life Sciences) after incubation with horseradish peroxidase-linked secondary antibodies (Dako A/S, Glostrup, Denmark). Quantification was performed by densitometric scanning using GS-710 software (Bio-Rad). Phosphoprotein levels were normalized calculating the ratio between phosphoprotein levels and total protein. In some cases, TNAP immunoreactivity was normalized to α-tubulin levels.

Immunocytochemistry—SH-SY5Y cells were fixed in 4% (v/v) paraformaldehyde for 15 min and washed three times with PBS. Before cells were treated with PBS/Triton X-100 containing 1% bovine serum albumin (BSA, w/v) for 45 min, coverslips were preincubated for 10 min with wheat germ agglutinin conjugated with Alexa Fluor 594 to stain the plasmatic membrane. Afterward, cells were incubated with antibodies against TNAP, and the catalytic subunits of PP2A were diluted 1:50 and 1:1000, respectively, in PBS/BSA and incubated for 45 min at room temperature. Subsequently, cells were rinsed with PBS and incubated with Alexa Fluor 488 anti-rabbit and Alexa Fluor 647 anti-mouse conjugated secondary antibodies (Invitrogen) diluted 1:500 in PBS/BSA. Finally, coverslips were extensively rinsed with PBS and mounted with FluorSave (Calbiochem). Analysis was performed by confocal microscopy on a Confocal MicroRadiance system (Bio-Rad) coupled to a vertical microscope, Axioskop 2 (Zeiss, Thornwood, NY).

Assay of TNAP Activity—TNAP activity was studied using two different experimental approaches. In the first one, a precipitating substrate of this enzyme named BCIP/NBT was employed, in accordance with manufacturer's recommendations (Sigma-Aldrich). This method allowed visualization of TNAP activity in cell membranes because BCIP/NBT precipitates and turns blue when it is dephosphorylated. In the second approach, TNAP activity was determined using a spectrophotometer. SH-SY5Y cells were homogenized with a Teflon glass homogenizer in 10 mM Tris-HCl buffer, pH 8.0, supplemented with 0.25 M sucrose and protease inhibitor mixture (EDTA-free Complete™, Roche Diagnostics) or with a protease inhibitor mixture containing 1 mM PMSF, 10 μg/ml aprotinin, 10 μg/ml leupeptin, and 50 μg/ml pepstatin. Aliquots of the homogenates were used as total fraction. Then, the homogenates were centrifuged at 9000 $\times$ *g* at 4 °C for 15 min, and the supernatants were centrifuged at 200,000 $\times$ *g* at 4 °C for 20 min using an Optima TL ultracentrifuge and a TLA100.4 rotor (Beckman). The pellets were solubilized in Tris-HCl buffer with 1% Triton X-100 (v/v) for 1 h at 4 °C (23). The supernatants and the solubilized membranes were used as cytosolic and membrane fractions, respectively. Aliquots from each fraction were assayed at 25 °C in the following reaction mix: 0.2 M diethanolamine buffer (Sigma-Aldrich), pH 9.8, 1 mM MgCl, and 5 mM *p*-nitrophenyl phosphate (Merck) in the presence or in the absence of 5 mM levamisole, an AP inhibitor. Reactions were stopped after 20 min with 0.1 M NaOH. Protein concentrations were quantified with the Bradford assay (24). AP activity was determined from the absorbance of the liberated *p*-nitrophenol at 405 nm and normalized to cellular protein content. The purity of the cytosolic and membrane fractions was checked by Western blotting using specific fraction markers such as Hsp90 and NMDA, respectively. AP activity was measured in total fractions of human brain samples.

Reverse Transcription-PCR Analysis—Total RNA was extracted from confluent SH-SY5Y cell cultures and human tissue using an RNA Minipreparation kit (Stratagene). RNA from 14 days *in vitro* cultured neurons was isolated using TRIzol (Invitrogen), following the manufacturer's instructions. After digestion with TURBO DNase (Ambion, Austin, TX), total RNA was quantified and reversed transcribed using a first-strand cDNA synthesis kit (AMV; Roche Diagnostics). Quantitative real-time PCR was performed using SYBR Green PCR Master Mix (Applied Biosystems) and gene-specific primers (150 nM) for the following genes: human β-actin, forward primer 5′-CACACTGTGCCCATCTACGA-3′ and reverse primer 5′-CTCCTTAATGTCACGCACGA-3′; human TNAP, forward primer 5′-CCATCCTGTATGGCAATGG-3′ and reverse primer 5′-CATGGAGACATTCTCTCGTTCA-3′; human M1 muscarinic receptor, forward primer 5′-ACCTCTATACCACGTACCTG-3′ and reverse primer 5′-TGAGCAGCAGATTCATGACG-3′; human M3 muscarinic receptor, forward primer 5′-CATCATGAATCGATGGGCCT-3′ and reverse primer 5′-GGCCTCGTGATGGAAAAGTA-3′; murine TNAP, forward primer 5′-ACTCAGGGCAATGAGGTCAC-3′ and reverse primer 5′-CACCCGAGTGGTAGTCACAA-3′; murine β-actin, forward primer 5′-GGCGCTTTTGACTCAGGATT-3′ and reverse primer 5′-GGGATGTTTGCTCCAACCAA-3′. Thermal cycling was performed using an ABI Prism 7900HT Sequence Detection system (Applied Biosystems) as follows: denaturation, one cycle of 95 °C for 10 min followed by 50 cycles each of 95 °C for 15 s and 60 °C for 1 min. Corresponding melting curves were analyzed to assess the specificity of the reaction. No-template reactions were used as negative controls, and reverse transcriptase minus-template reactions were performed to rule out genomic DNA contamination. β-Actin was used as an endogenous control to normalize differences in mRNA amounts.

Microfluorometric Calcium Assays—SH-SY5Y human neuroblastoma cells were washed with perfusion buffer (122 mM NaCl, 3.1 mM KCl, 0.4 mM KH_2PO_4, 5 mM $NaHCO_3$, 1.2 mM $MgSO_4$, 10 mM glucose, and 20 mM TES buffer, pH 7.4), and they were then loaded with the calcium dye FURA-2 AM (7.5 μM) for 30 min at 37 °C. This incubation facilitated the intracellular hydrolysis of the FURA-2 AM. Subsequently, the coverslips were washed with fresh medium and mounted in a superfusion chamber on a NIKON Eclipse TE-2000 microscope (Nikon, Japan). In all experiments, cells were first superfused at 1.2 ml/min with perfusion medium before acetylcholine (ACh; used as a control to assess the functional status of the cells) or 100 nM tau was assayed. At the end of each experiment, 10 μM ACh pulses were applied to confirm the viability of the studied cells. Cells were visualized using a Nikon microscope using a $\times$40 S Fluor 0.5–1.3 oil lens. The wavelength of the incoming light was filtered to 340 nm and 380 nm with the aid of a monochromator (10 nm bandwidth, Optoscan monochromator; Cairin), wavelengths that corresponded to the fluorescence peaks of the Ca^{2+}-saturated and Ca^{2+}-free FURA-2 solutions. The 12-bit images were acquired with an ORCA-ER C 47 42–98 CCD camera from Hamamatsu (Hamamatsu City, Japan) controlled by Metafluor 6.3r6 PC software (Universal Imaging Corp., Cambridge, UK). The exposure time was 250 ms at each wavelength, and the changing time was 5 ms. Images were acquired continuously and buffered in a fast SCSI disk. Time course data represent the average light intensity in a small elliptical region inside each cell. The background and autofluorescence components were subtracted at each wavelength, and the 340:380 nm ratio was calculated (25).

Statistical Analyses—Data are always presented as mean ± S.D., and the number of experiments (*n*) is indicated. Statistical analyses were performed using Student's *t* test to compare group mean. In all analyses, the null hypothesis was rejected at >0.05.

RESULTS

Exogenous Tau Peptide 3RC Induces Intracellular Tau Phosphorylation and Cell Death—Previously, we reported that tau protein interacts with M1 and M3 muscarinic membrane receptors located at the cell surface leading to an increase in the levels of intracellular calcium concentration and the phosphorylation of intracellular tau at non–proline-directed phosphorylatable sites (9). The same effect is mediated tau3RC peptide. In this work, we have tested whether upon addition of extracellular tau intracellular tau can be also modified at proline-directed phosphorylatable sites. To do that, we have used the peptide tau3RC. Tau3RC is a peptide lacking the N-terminal region of tau protein, and it has been reported to be toxic for cultured SH-SY5Y cells (7). Thus, SH-SY5Y cells were stimulated with vehicle (control cells) or tau3RC for 48 h, and the levels of intracellular tau were measured in cellular extracts by Western blotting using Tau-1 antibody that recognizes unphosphorylated tau at Ser^{198}, Ser^{199}, and Ser^{202} (serines followed by prolines). As shown in Fig. 1, a decrease in unphosphorylated tau protein was observed after tau3RC treatment, suggesting that intracellular tau is highly phosphorylated at the sequence recognized by Tau-1 antibody.

Exogenous Tau Promotes the Release of Intracellular Tau at the Extracellular Medium—To determine whether endogenous tau is located in the extracellular medium following cell death, SH-SY5Y cells were treated with vehicle or tau3RC for 48 h. Afterward, tau levels were analyzed in the culture medium by Western blotting using either Br133 antibody, which recognizes N-terminal region of endogenous tau but not tau3RC, or Tau-1 antibody, which binds to an amino acid sequence present in the proline-rich region of tau molecule that is absent in tau3RC peptide (Fig. 2*A*). Both antibodies clearly demonstrated that exogenous tau treatment is able to increase extracellular tau levels compared with control cells (Fig. 2, *B* and *C*). No significant differences between control and treated cells were observed when Tau-5, a phosphate-independent antibody that recognizes both tau3RC and endogenous tau, was employed (Fig. 2*D*).

The increase in extracellular tau detected by the Tau-1 antibody could be also explained by a lower degree of phosphorylation of extracellular tau because Tau-1 antibody recognizes phosphorylatable Ser residues but in their dephosphorylated form. Taking into account that tau3RC treatment increases intracellular tau phosphorylation (Fig. 1*D*), we tested whether dephosphorylation occurs once it reaches extracellular media.

Tau Is Dephosphorylated in the Extracellular Medium—To know whether endogenous tau is dephosphorylated in the extracellular medium, SH-SY5Y cells were treated with vehicle or tau3RC for 48 h. Then, the levels of phosphorylated tau found in the culture medium were analyzed by Western blotting using AT8 antibody, which recognizes a sequence similar to Tau-1 but in a phosphorylated state, and PHF1 antibody that binds to a phosphorylated sequence located closed to the C terminus of tau protein

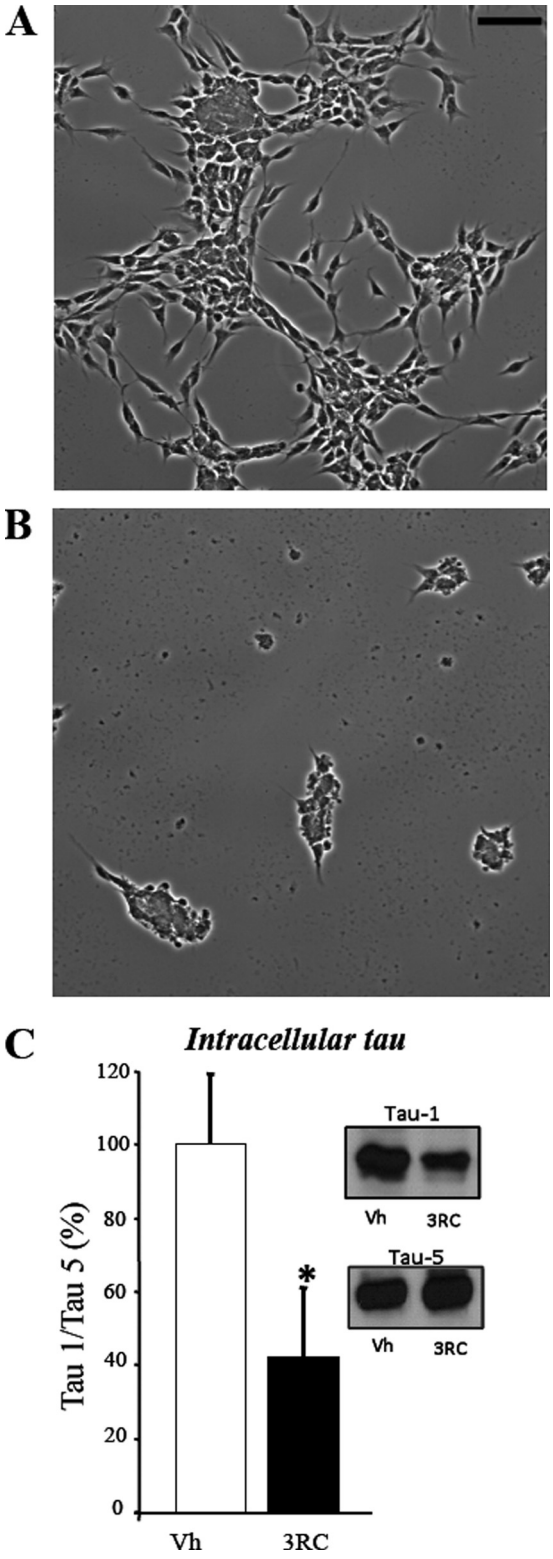

FIGURE 1. **Extracellular tau3RC peptide promotes endogenous tau phosphorylation.** *A* and *B*, representative images of SH-SY5Y human neuroblastoma cells treated for 48 h with vehicle solution (*A*) or with 1 μM tau3RC peptide (*B*) are shown. *Scale bar*, 50 μm. A clear morphological change was found upon tau peptide addition. *C*, cellular extracts from SH-SY5Y stimulated with vehicle (*Vh*) or with tau3RC (*3RC*; 1 μM for 48 h) were analyzed by Western blotting using Tau-1 antibody. Protein bands were scanned and normalized to Tau-5 level. 100% corresponds with the ratio tau-1/tau-5 obtained in vehicle-treated SH-SY5Y cells. *Graph* represents the mean ± S.D. (*error bars*) from three individual experiments. *, $p < 0.05$.

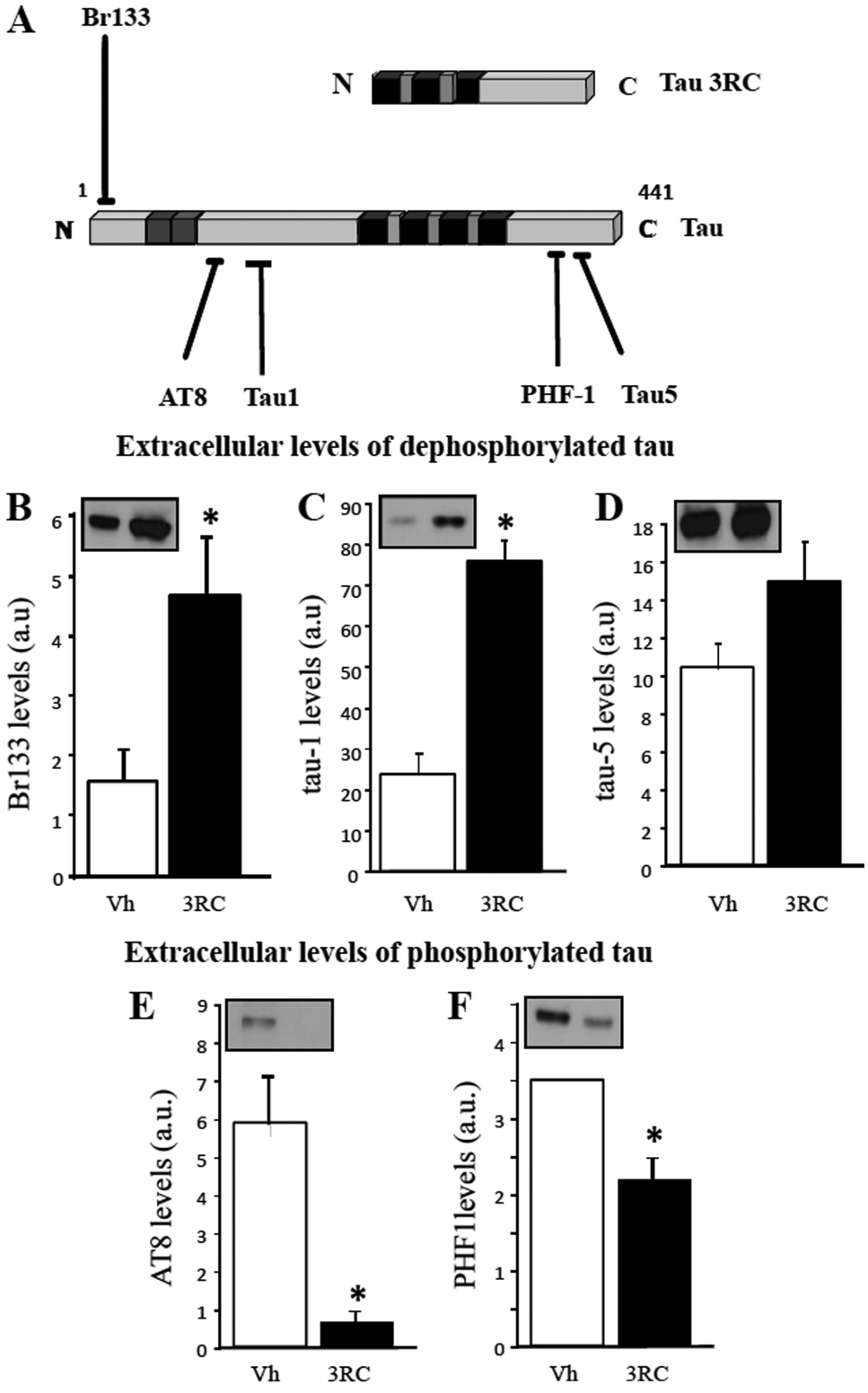

FIGURE 2. **Extracellular tau promotes the release of intracellular tau, which is dephosphorylated in the extracellular medium.** *A*, schematic representation of tau species and antibodies used in these experiments is shown. *Black blocks* represent the tubulin binding repeats; *gray blocks* represent exons 2 and 3. BR133 antibody recognizes the N terminus of tau, and Tau-1 antibody recognizes unphosphorylated Ser^{198}, Ser^{199}, Ser^{202}. AT8 antibody recognizes tau when phosphorylated at Ser^{202} and Thr^{205}. These antibodies recognize endogenous tau, but not tau3RC. Tau-5 is a phosphate-independent antibody that recognizes both endogenous tau and tau3RC, whereas PHF1 antibody requires phosphorylated tau at Ser^{396}, Ser^{404} residues (17). *B–D*, culture medium from cells treated with vehicle solution (*Vh*) or with 1 μM tau3RC for 48 h was collected, and extracellular tau levels were measured by Western blotting using Br133 (*B*), Tau-1 (*C*), and Tau-5 (*D*) antibodies. *Graphs* represent the mean ± S.D. (*error bars*) from three individual experiments. *, $p < 0.05$. *E* and *F*, levels of extracellular phosphorylated tau were also measured by Western blotting using antibodies that specifically recognized the phosphorylated epitopes of tau protein, AT8 (*E*) and PHF1 (*F*). Blots were scanned to determine the proportion of phosphorylated tau. *Graphs* represent the mean ± S.D. from three individual experiments. *a.u.*, arbitrary units. *, $p < 0.05$.

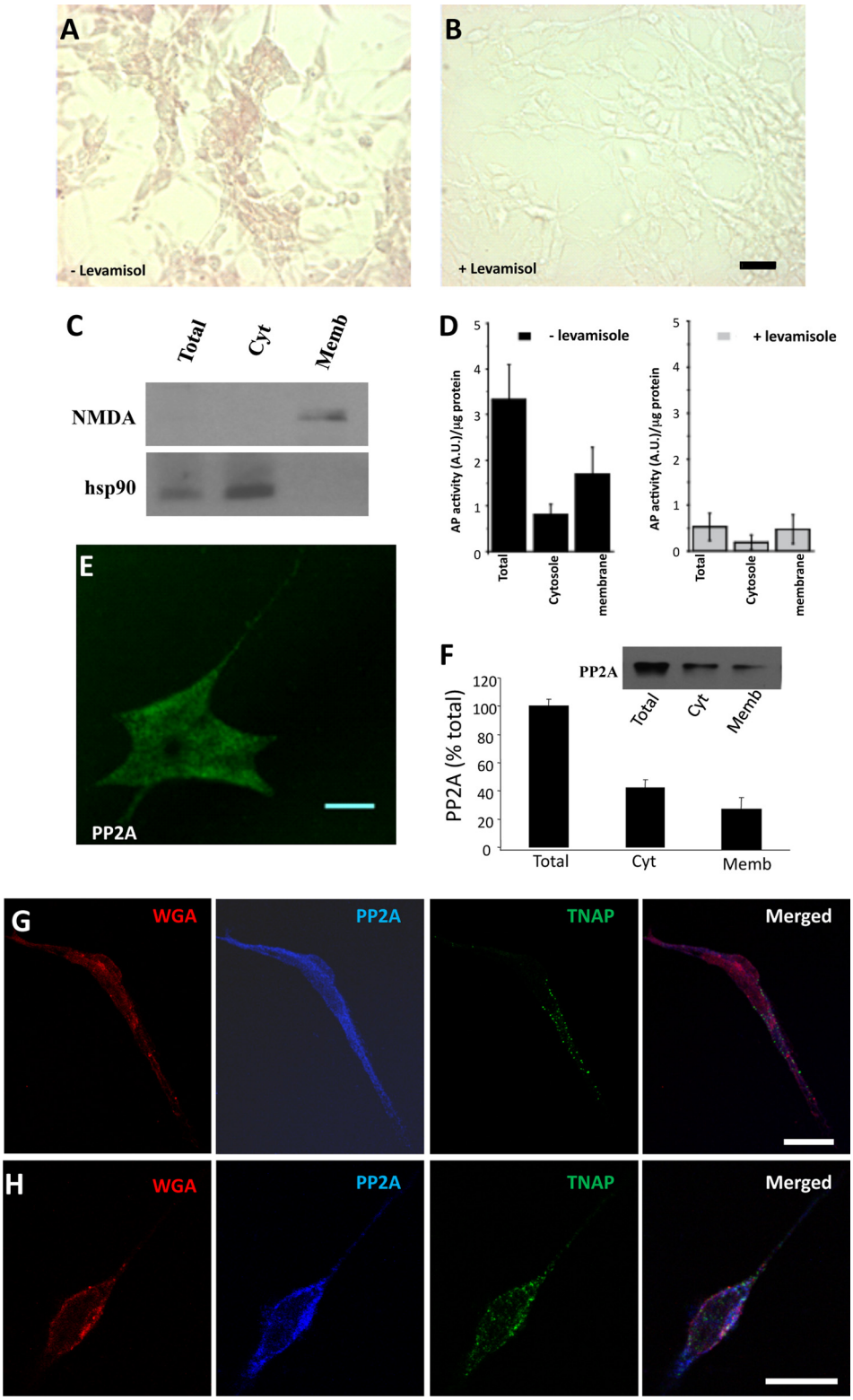

FIGURE 3. **Location of TNAP in SH-SY5Y cells.** *A* and *B*, optical images of nonpermeabilized SH-SY5Y cells fixed and incubated with BCIP/NBT (a TNAP substrate that precipitates and turns violet/blue when dephosphorylated) in the absence (*A*) or presence (*B*) of 1 mM levamisole, a specific inhibitor of TNAP, for 1 h. *Scale bar*, 50 μm. It should be indicated that TNAP activity remains in the fixed cells. *C* and *D*, measurement of TNAP activity in total, cytosolic (*Cyt*), and membrane (*Memb*) fractions from SH-SY5Y cells using *p*-nitrophenyl phosphate as a substrate of the enzyme. *C*, purity of cytosolic and membrane fractions assessed by Western blotting using specific fraction markers such as Hsp90 and NMDA, respectively. *D*, graph representing the mean ± S.D. (*error bars*) from three individual experiments. *E* and *F*, confocal fluorescence image of fixed SH-SY5Y cell stained with an antibody that recognizes the catalytic subunit of PP2A. *Scale bar*, 10 μm. *F inset*, Western blot using PP2A antibody in total, cytosolic, and membrane fractions from SH-SY5Y cells. *Graph*, mean ± S.D. from three individual experiments. *G* and *H*, confocal fluorescence images of fixed SH-SY5Y cells stained with the plasma membrane marker wheat germ agglutinin (*WGA*) (*red*) and with antibodies against PP2A (*blue*) and TNAP (*green*). *Merged image* is showed in the last panel. *Scale bar*, 25 μm.

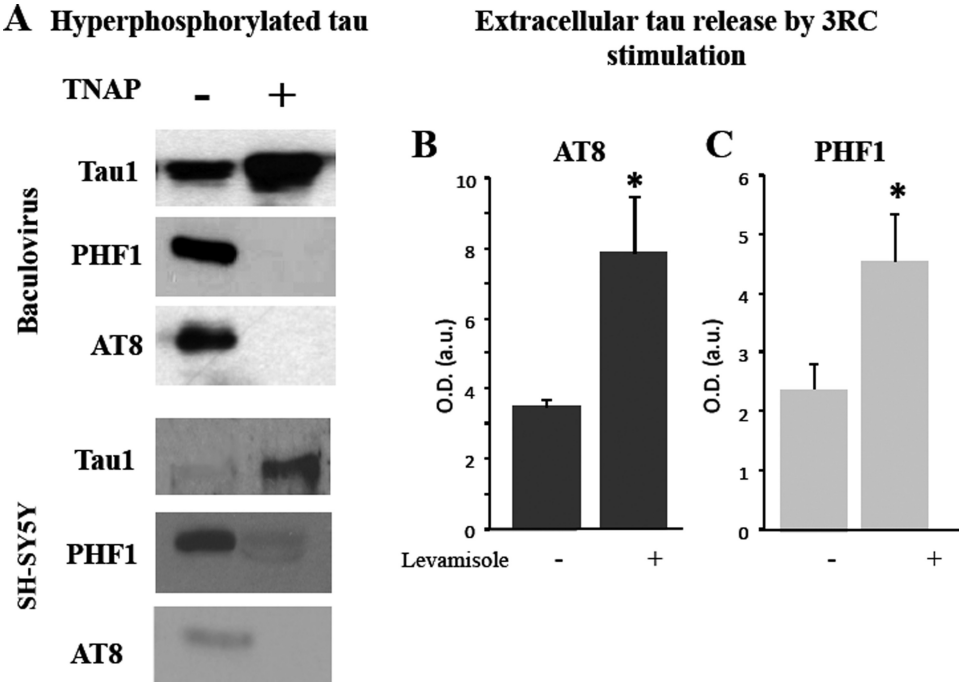

FIGURE 4. **TNAP dephosphorylates phospho-tau.** *A*, several samples of hyperphosphorylated tau obtained from an insect cell culture infected with baculovirus expressing tau protein (*upper panel*) or phospho intracellular tau protein from SY5Y cells (*lower panel*) were incubated in the presence (+) or absence (−) of TNAP for 1 h at 37 °C. Phosphorylation degree of those samples were analyzed by Western blotting using Tau-1, PHF1, and AT8 antibodies. *B* and *C*, phosphorylation levels of endogenous tau released from tau3RC-treated cells (*3RC*; 1 μM for 48 h) in the presence or absence of 1 mM levamisole are shown. Culture media were collected, and extracellular tau levels were measured by dot-blotting using AT8 (*B*) and PHF1 (*C*) antibodies. *Graph* represents the mean ± S.D. (*error bars*) from three individual experiments. *, $p < 0.05$.

(Fig. 2*A*). In both cases, a decrease in tau phosphorylation was observed after tau3RC treatment (Fig. 2, *E* and *F*), demonstrating that intracellular tau undergoes a broad dephosphorylation once it is present at the extracellular medium likely due to the action of cell membrane phosphatases. A well known example of these enzymes is TNAP, which is located not only in the cytosol but also in the membrane of neuronal cells (26).

Presence of Functional TNAP in Neuroblastoma Cells—The presence of functional TNAP in SH-SY5Y cells was confirmed by several methods: (i) detection of TNAP activity in intact cells using BCIP/NBT, a substrate of TNAP that precipitates and turns violet/blue when it is dephosphorylated (Fig. 3, *A* and *B*); (ii) measurement of TNAP activity in subcellular fractions using *p*-nitrophenyl phosphate as a substrate of this enzyme (Fig. 3, *C* and *D*); and (iii) immunocytochemical detection of TNAP in neuroblastoma cells using specific antibodies (Fig. 3, *G* and *H*). Cellular fractioning was verified using NMDA receptor antibody as a membrane fraction marker and Hsp90 antibody as a marker of cytosolic fraction (Fig. 3*C*). Alkaline phosphatase activity was quantified in alkaline conditions (pH 9.8) in the absence or presence of levamisole. Under these experimental conditions, the levamisole-sensitive alkaline phosphatase activity corresponds to TNAP activity. Interestingly, the highest proportion of TNAP activity in the neuroblastoma cells was detected in the membrane fraction (Fig. 3*D*). In good agreement with these results immunocytochemical studies revealed that TNAP is mainly co-localized with the plasma membrane marker wheat germ agglutinin in SH-SY5Y cells (Fig. 3, *G* and *H*). As a control we have tested the localization of a major tau phosphatase, PP2A (27), a protein that was located mainly in the cytosol of SH-SY5Y cells (Fig. 3, *E–H*).

TNAP Is Able to Dephosphorylate Phospho-tau—Incubation of phospho-tau (obtained by two different ways: tau-expressing baculovirus-infected insect cells (21) or intracellular phospho-tau from SH-SY5Y cells) with exogenous TNAP resulted in a widespread dephosphorylation of phospho-tau, as indicated by a decrease in the band recognized by AT8 and PHF1 antibodies and an increase in the band recognized by Tau-1 antibody (Fig. 4*A*). Pretreatment with the TNAP inhibitor 1 mM levamisole for 1 h completely prevented phospho-tau dephosphorylation in the extracellular medium (Fig. 4, *B* and *C*). These results strongly suggest that TNAP is the phosphatase involved in the dephosphorylation of intracellular tau, once it is released at the extracellular space.

Extracellular Dephosphorylated Tau Elicits a Greater Increase in Intracellular Calcium Concentration than Phosphorylated Tau—The next question was whether the tau phosphorylation degree is somehow regulating the release of calcium from intracellular stores increase induced by extracellular tau in neuronal cells (7, 9). The stimulation of SH-SY5Y cells with unphosphorylated tau (100 nM) led to a significant increase in intracellular calcium levels, whereas hyperphosphorylated tau did not produce any noticeable effect (Fig. 5*A*). Moreover, co-application of both TNAP and phospho-tau produce a calcium increase comparable with that observed with unphosphorylated tau, demonstrating once more that dephosphorylation of phospho-tau by TNAP is required for the induction of calcium increase (Fig. 5*B*). In a previous work, it has been reported that the toxic effect of tau on neuronal cells may be due to the presence of a small peptide (residues 391–407) integrated into the tau molecule. Interestingly, we observed that this peptide can induce an increase in intracellular calcium in neuroblastoma cells, an effect that is prevented when this peptide is phosphorylated at Ser^{396} and Ser^{404} (Fig. 5*C*). This phosphorylation can be specifically recognized by PHF1 antibody (17).

Intracellular Calcium Increments, Induced by Unphosphorylated Tau, Modulate TNAP Expression in SH-SY5Y Cells—SH-SY5Y cells were treated with vehicle or unphosphorylated tau for 48 h, and TNAP levels were analyzed by Western blotting. As shown in Fig. 6*A*, TNAP levels were significantly enhanced after tau treatment, suggesting that the tau-induced increase in intracellular calcium somehow regulates the expression of the enzyme (Fig. 6, *A* and *B*).

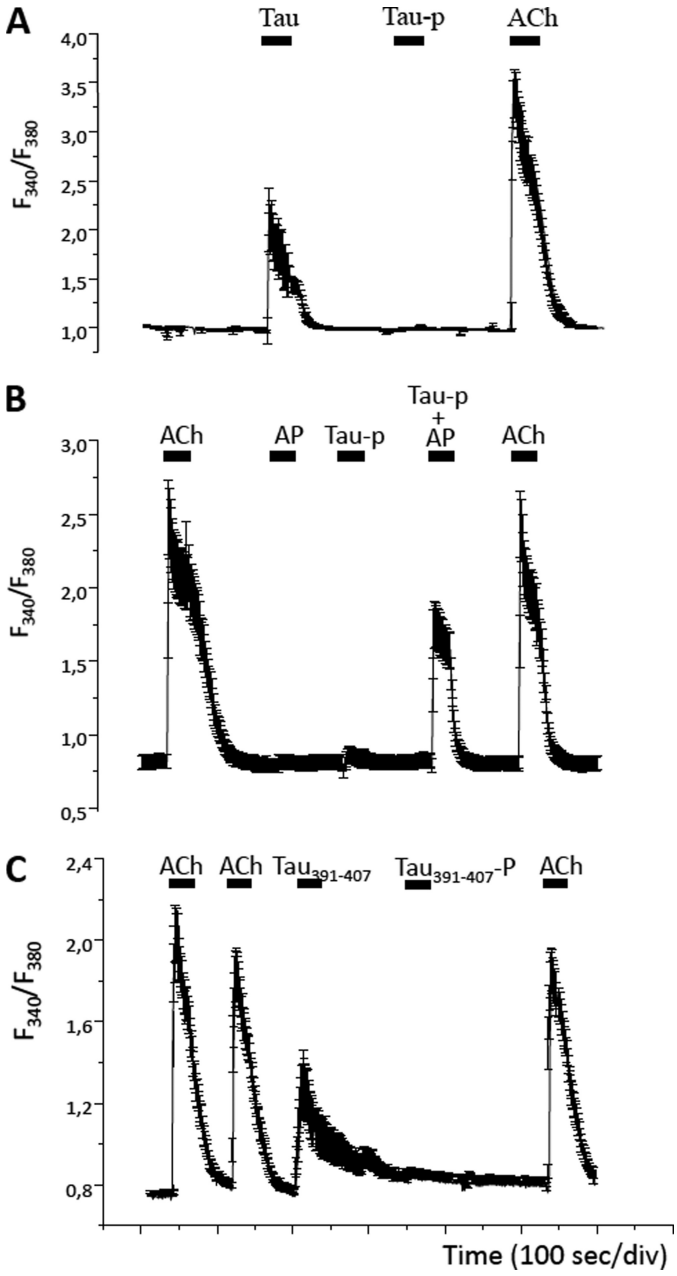

FIGURE 5. **Effect of hyperphosphorylated and unphosphorylated tau on the intracellular calcium concentration in SH-SY5Y cells.** *A*, SH-SY5Y cells loaded with the calcium dye FURA-2 (see "Experimental Procedures") were superfused with 100 nM unphosphorylated (*Tau*) or phosphorylated tau (*Tau-p*), and their effect in intracellular calcium concentration was measured. At the end of the experiment, cells were stimulated with a pulse of 10 μM ACh to determine the functional status of each cell. *B*, SH-SY5Y cells loaded with FURA-2 were sequentially stimulated with 10 μM ACh, 1 mM TNAP, phosphorylated tau, and TNAP-treated phosphorylated tau (*Tau-p + TNAP*). The dephosphorylated tau retrieves the increase in the intracellular calcium concentration provoked by tau. At the end of the experiment, cells were stimulated with a pulse of 10 μM ACh to determine the functional status of each cell. *C*, SH-SY5Y cells loaded with FURA-2 were sequentially stimulated with 10 μM ACh, 100 nM $Tau_{391-407}$, and $Tau_{391-407}$-P (same peptide but phosphorylated in all Ser residues). A final pulse of 10 μM ACh was applied at the end of the experiment. *Traces* show the average of ≥20 cells, and the *error bars* indicate the S.D. In all cases, *upper solid bars* indicate the stimulation periods.

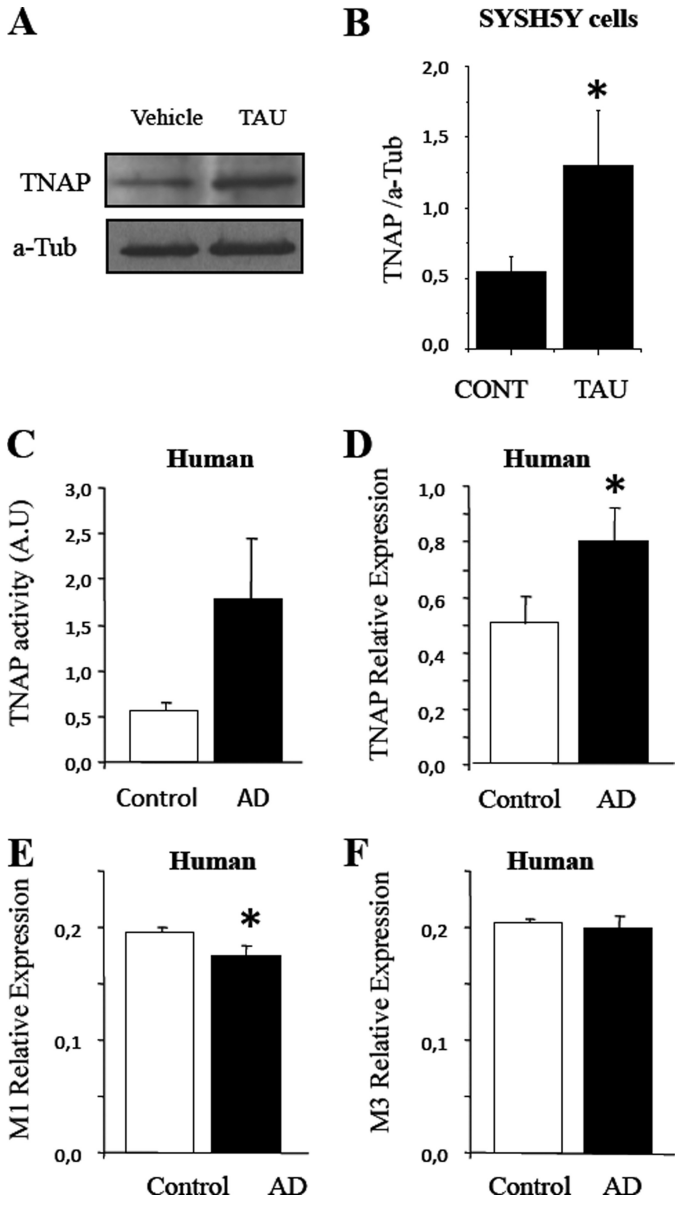

FIGURE 6. **TNAP expression is increased in different cell systems.** *A*, cellular extracts from SH-SY5Y cells treated with vehicle solution (*Vehicle* or *CONT*) and with 1 μM unphosphorylated tau (*TAU*) for 5 days were analyzed by Western blotting using a specific antibody against TNAP. *B*, protein bands were scanned and were normalized to α-tubulin level ($n = 4$); *, $p < 0.05$. *C*, TNAP activity was measured in frozen brain samples from either healthy (control) or AD patients by using *p*-nitrophenyl phosphate as a substrate of the enzyme. *D–F*, relative expression of TNAP (*D*), M1 (*E*) and M3 (*F*) muscarinic receptor mRNA in the brain of healthy and AD patients is represented. β-Actin transcript was used as an endogenous control to normalize differences in total RNA amounts ($n = 6$ for controls and $n = 6$ for AD). *, $p < 0.05$. In all cases, *error bars* represent the S.D.

Brains from AD Patients Show an Increase in TNAP Activity—Previous findings indicate that extracellular unphosphorylated tau produces an increase in intracellular calcium levels and a subsequent increase in TNAP expression. Thus, we have tested whether a similar effect could be observed in the brain of AD patients. As shown in Fig. 6, *C* and *D*, respectively, both the activity and the expression of TNAP were enhanced in the temporal gyrus of AD patients compared with nondiseased donors (Table 1). A slight decrease in the expression of M1 muscarinic receptors in AD patients was also observed (Fig. 6*E*), although no changes in the expression of M3 muscarinic receptors were found (Fig. 6*F*).

DISCUSSION

In the present work, we have shown that intracellular phospho-tau is released to the extracellular space by extracellular tau-induced muscarinic receptor activation. In this location, tau is dephosphorylated by extracellular TNAP anchored in the cellular membrane. Extracellular dephosphorylated tau is able to interact with muscarinic receptors M1 and M3 located on the surface of neighboring cells, inducing their death (7). However, in this slow neurotoxic process (7–9), distinct intracellular pathways are activated before cell death. As previously reported, intracellular calcium levels are increased in the cytosolic compartment, and calcium-dependent protein kinases are activated, inducing tau phosphorylation (9). Furthermore, here we report that TNAP expression is regulated by the action of extracellular tau (28). Thus, we have identified a new component (TNAP) that mediates the neurotoxicity cycle induced by extracellular monomeric tau.

TNAP plays a pivotal role in the neurotoxic effect of extracellular tau, transforming this protein into a muscarinic receptor agonist by means of its dephosphorylation. The higher expression and activity levels of this enzyme found in postmortem brain of AD patients confirm its participation on the progression of AD.

Recent studies have described extracellular interactions of tau in its aggregated form with neuronal cells (6, 29). Aggregated tau can be endocytosed into the cell, promoting a further aggregation of intracellular tau, exerting a prion protein-like behavior (6, 29). However, we did not observe any effects on neurons treated with aggregated tau forms (9). These apparently contradictory effects can be explained taking into account the time course required for each phenomenon. Whereas the neurotoxic effect of extracellular monomeric tau mediated by muscarinic receptors occurs within 2 days (7), the prion protein-like behavior of aggregated tau requires months (29). We postulate that the longer time course of the prion effect of aggregated tau could be the result of accumulated effects of the neurotoxicity cycle of monomeric tau. However, we do not rule out that both are independent phenomena that contribute to the spread of AD pathology.

Two mechanisms for the release of intracellular tau into the extracellular space have been proposed. One possibility is that tau is secreted through microvesicles (6), as previously suggested for intracellular α-synuclein, which may be secreted in a calcium-dependent manner by exosomes (30). A second possibility is that soluble tau may be released from the neuron upon cell death. This tau could promote an increase in intracellular calcium, resulting in cell death and consequently, further release of intracellular tau (7–9). In both cases, extracellular toxic tau is present and should be removed to ensure cell survival. Recently, the feasibility of a tau immunotherapeutic approach has been suggested (31, 32).

In general, it could be considered that intracellular phospho-tau could be toxic inside the cells (33, 34), whereas the extracellular toxic effect of tau occurs with the unphosphorylated protein. After neurodegeneration and neuronal death, higher levels of extracellular tau will be present in a unphosphorylated form in the extracellular matrix, and a new neurodegeneration cycle could take place. This mechanism has been proposed (7, 9, 33) to explain the propagation of tau pathology that occurs in AD from the hippocampal region, the earliest to be affected (35, 36), to the cortex. This possible role of tau itself in the propagation of its pathology is in good agreement with the increase in neurodegeneration found in a transgenic mouse model overexpressing tau protein (37). We propose now a new role for TNAP in the toxic effect of extracellular tau protein that requires that extracellular tau remain in a dephosphorylated state. This hypothesis is compatible with TNAP distribution in the brain because a relatively high proportion of the enzyme is located in the hippocampus and in the cortex. Interestingly, the tau domain involved in the interaction of monomeric tau with cell surface receptors (7) contains an amino acid sequence that is recognized by PHF1 antibody when phosphorylated. It must be noted that PHF1 antibody binds strongly to aggregated tau filaments and not to dephosphorylated tau (38). Thus, further studies are required to understand fully the different roles played by extracellular tau, in aggregated or monomeric form, in cell degeneration.

Acknowledgments—We thank The Netherlands Brain Bank (Coordinator Dr. I. Huitinga) for provision of the human brain material and Dr. O. Howard for the critical reading of the manuscript.

REFERENCES

1. Grundke-Iqbal, I., Iqbal, K., Tung, Y. C., Quinlan, M., Wisniewski, H. M., and Binder, L. I. (1986) *Proc. Natl. Acad. Sci. U.S.A.* **83,** 4913–4917
2. Braak, H., and Braak, E. (1991) *Acta Neuropathol.* **82,** 239–259
3. Fukutani, Y., Kobayashi, K., Nakamura, I., Watanabe, K., Isaki, K., and Cairns, N. J. (1995) *Neurosci. Lett.* **200,** 57–60
4. Cras, P., Smith, M. A., Richey, P. L., Siedlak, S. L., Mulvihill, P., and Perry, G. (1995) *Acta Neuropathol.* **89,** 291–295
5. Bondareff, W., Mountjoy, C. Q., Roth, M., and Hauser, D. L. (1989) *Neurobiol. Aging* **10,** 709–715
6. Frost, B., Jacks, R. L., and Diamond, M. I. (2009) *J. Biol. Chem.* **284,** 12845–12852
7. Gómez-Ramos, A., Díaz-Hernández, M., Rubio, A., Miras-Portugal, M. T., and Avila, J. (2008) *Mol. Cell. Neurosci.* **37,** 673–681
8. Gómez-Ramos, A., Díaz-Hernández, M., Rubio, A., Díaz-Hernández, J. I., Miras-Portugal, M. T., and Avila, J. (2009) *Eur. Neuropsychopharmacol.* **19,** 708–717
9. Gómez-Ramos, A., Díaz-Hernández, M., Cuadros, R., Hernández, F., and Avila, J. (2006) *FEBS Lett.* **580,** 4842–4850
10. Robson, S. C., Sévigny, J., and Zimmermann, H. (2006) *Purinergic Signal.* **2,** 409–430
11. Zimmermann, H. (2006) *Novartis Found. Symp.* **276,** 113–130, 233–237, 275–281
12. Zimmermann, H. (2000) *Naunyn Schmiedebergs Arch. Pharmacol.* **362,** 299–309
13. Ogata, S., Hayashi, Y., Takami, N., and Ikehara, Y. (1988) *J. Biol. Chem.* **263,** 10489–10494
14. Henthorn, P. S., Raducha, M., Fedde, K. N., Lafferty, M. A., and Whyte, M. P. (1992) *Proc. Natl. Acad. Sci. U.S.A.* **89,** 9924–9928
15. Anderson, H. C., Sipe, J. B., Hessle, L., Dhanyamraju, R., Atti, E., Camacho, N. P., Millán, J. L., and Dhamyamraju, R. (2004) *Am. J. Pathol.* **164,** 841–847
16. Andorfer, C., Acker, C. M., Kress, Y., Hof, P. R., Duff, K., and Davies, P. (2005) *J. Neurosci.* **25,** 5446–5454
17. Otvos, L., Jr., Feiner, L., Lang, E., Szendrei, G. I., Goedert, M., and Lee,

V. M. (1994) *J. Neurosci. Res.* **39,** 669–673
18. Biedler, J. L., Roffler-Tarlov, S., Schachner, M., and Freedman, L. S. (1978) *Cancer Res.* **38,** 3751–3757
19. Pérez, M., Valpuesta, J. M., Medina, M., Montejo de Garcini, E., and Avila, J. (1996) *J. Neurochem.* **67,** 1183–1190
20. Goedert, M., Spillantini, M. G., Jakes, R., Rutherford, D., and Crowther, R. A. (1989) *Neuron* **3,** 519–526
21. Gómez-Ramos, A., Abad, X., López Fanarraga, M., Bhat, R., Zabala, J. C., and Avila, J. (2004) *Brain Res.* **1007,** 57–64
22. Correas, I., Díaz-Nido, J., and Avila, J. (1992) *J. Biol. Chem.* **267,** 15721–15728
23. Iwata, N., Takaki, Y., Fukami, S., Tsubuki, S., and Saido, T. C. (2002) *J. Neurosci. Res.* **70,** 493–500
24. Bradford, M. M. (1976) *Anal. Biochem.* **72,** 248–254
25. Díaz-Hernández, M., Pintor, J., Castro, E., and Miras-Portugal, M. T. (2001) *Eur. J. Neurosci.* **14,** 918–926
26. Fonta, C., Négyessy, L., Renaud, L., and Barone, P. (2004) *Cereb. Cortex* **14,** 595–609
27. Gong, C. X., and Iqbal, K. (2008) *Curr. Med. Chem.* **15,** 2321–2328
28. Carrión, A. M., Link, W. A., Ledo, F., Mellström, B., and Naranjo, J. R. (1999) *Nature* **398,** 80–84
29. Clavaguera, F., Bolmont, T., Crowther, R. A., Abramowski, D., Frank, S., Probst, A., Fraser, G., Stalder, A. K., Beibel, M., Staufenbiel, M., Jucker, M., Goedert, M., and Tolnay, M. (2009) *Nat. Cell Biol.* **11,** 909–913
30. Emmanouilidou, E., Melachroinou, K., Roumeliotis, T., Garbis, S. D., Ntzouni, M., Margaritis, L. H., Stefanis, L., and Vekrellis, K. (2010) *J. Neurosci.* **30,** 6838–6851
31. Asuni, A. A., Boutajangout, A., Quartermain, D., and Sigurdsson, E. M. (2007) *J. Neurosci.* **27,** 9115–9129
32. Boimel, M., Grigoriadis, N., Lourbopoulos, A., Haber, E., Abramsky, O., and Rosenmann, H. (2010) *Exp. Neurol.* **224,** 472–485
33. Gómez de Barreda, E., Pérez, M., Gómez Ramos, P., de Cristobal, J., Martin-Maestro, P., Moran, A., Dawson, H. N., Vitek, M. P., Lucas, J. J., Hernandez, F., and Avila, J. (2010) *Neurobiol. Dis.* **37,** 622–629
34. Avila, J., Lucas, J. J., Perez, M., and Hernandez, F. (2004) *Physiol. Rev.* **84,** 361–384
35. Braak, H., and Braak, E. (1996) *Acta Neurol. Scand. Suppl.* **165,** 3–12
36. Braak, H., and Braak, E. (1985) *Acta Neuropathol.* **68,** 325–332
37. Engel, T., Lucas, J. J., Gómez-Ramos, P., Moran, M. A., Avila, J., and Hernández, F. (2006) *Neurobiol. Aging* **27,** 1258–1268
38. Greenberg, S. G., and Davies, P. (1990) *Proc. Natl. Acad. Sci. U.S.A.* **87,** 5827–5831